Particle precipitation in connection with KOH etching of silicon

Nielsen, Christian Bergenstof; Christensen, Carsten; Pedersen, Casper; Thomsen, Erik Vilain

Published in:
Journal of The Electrochemical Society

Link to article, DOI:
10.1149/1.1688802

Publication date:
2004

Document Version
Publisher's PDF, also known as Version of record

Journal of The Electrochemical Society, **151** (5) G338-G342 (2004)
0013-4651/2004/151(5)/G338/5/$7.00 © The Electrochemical Society, Inc.

Particle Precipitation in Connection with KOH Etching of Silicon

C. Bergenstof Nielsen,[z] C. Christensen, C. Pedersen, and E. V. Thomsen

Mikroelektronik Centret, The Technical University of Denmark, 2800 Lyngby, Denmark

This paper considers the precipitation of iron oxide particles in connection with the KOH etching of cavities in silicon wafers. The findings presented in this paper suggest that the source to the particles is the KOH pellets used for making the etching solution. Experiments show that the precipitation is independent of KOH etching time, but that the amount of deposited material varies with dopant type and dopant concentration. The experiments also suggest that the precipitation occurs when the silicon wafers are removed from the KOH etching solution and not during the etching procedure. When not removed, the iron oxide particles cause etch pits on the Si surface when later processed and exposed to phosphoric acid. It has been found that the particles can be removed in an HCl solution, but not completely in an H_2SO_4-H_2O_2 solution. The paper discusses the involved precipitation mechanism in terms of the change in free energy of adsorption, the Pourbaix diagram, the electrochemical double-layer thickness and silicon dopant type, and concentration.
 [DOI: 10.1149/1.1688802]

Manuscript received April 28, 2003. Available electronically March 23, 2004.

KOH etching is widely used in connection with micromachining of microelectromechanical systems (MEMS). As an example, in the manufacturing of pressure sensors, an-isotropic KOH etching of silicon is used for making pressure sensitive membranes. Making a silicon membrane using KOH etching involves a six-step procedure. (*i*) Silicon nitride is deposited on a 4 in. silicon wafer. (*ii*) The silicon nitride is oxidized. (*iii*) Using photoresist in a standard photolithography technique, mask holes are defined in the silicon oxide using a HF etching solution. (*iv*) The silicon nitride is now exposed to phosphoric acid at $T = 180°C$ where the unmasked areas are removed. In this process step, silicon oxide is not etched. (*v*) The silicon wafer with a silicon nitride mask is then exposed to a KOH etching solution, where unmasked silicon is removed. Membranes are formed when sufficient material has been etched away. This etching will also typically remove the silicon oxide mask. (*vi*) The nitride mask is finally removed in phosphoric acid. In the case of normal conditions the phosphoric acid will not etch the exposed silicon.

The motivation for this work was initiated by the discovery of iron oxide particles found on the silicon membrane and sidewalls of the cavity after such an anisotropic KOH etching of pressure sensors. Figure 1 shows such a particle contamination at 10,000 times magnification and Fig. 2 shows at a higher magnification a chain of these particles. Furthermore, it turned out that the KOH etching procedure did not deposit particles on either SiO_2 or on Si_3N_4 masking layers, and when performing step (*vi*) in the procedure described above, the particles were not removed. Instead they caused pits in the silicon where particles were situated. In Fig. 3 a silicon membrane with particles and pits is shown. Both the presence of etch pits and particles is detrimental to sensors working in harsh environments since a coating with a passivating layer becomes difficult if not impossible.[1] Evidently the presence of iron particles is also detrimental to MEMS sensors since the iron will alter the behavior of the electronics that is present on the device.[2]

The work presented here focuses on precipitation mechanisms and on how the contaminated silicon surface can be cleaned satisfactory.

The presence of metal contamination of KOH etching solutions has been the subject of investigations before,[3-7] however, to the best of our knowledge, the presence of metal oxides on silicon wafers, the amount, the individual particle size, and morphology has never before been described.

[z] E-mail: cbn@mic.dtu.dk

Experimental

Three experiments have been performed. Experiment I was designed to establish whether or not particle size and number grow with etching time. Experiment II was designed to give additional information on the technological aspect of wafer etching in the case of different dopant types and dopant levels, and experiment III was designed to investigate particle removal. In both experiment I and II the involved silicon(100) wafers were oxide stripped in a buffered HF etch for 30 s and subsequently rinsed in a deionized H_2O rinsing solution (with a resistivity of 18 MΩ cm) with N_2 bubbling for 3 min, prior to the KOH etching solution exposure. This was done in order to remove the native oxide from the silicon wafers, and thus ensure equal initial etching conditions. The KOH etching solution parameters are also common to experiment I and II, namely (*i*) the wafers are etched in an upright position in the etching solution, with the flat pointing upwards. The flat is a marker that is used to identify the [100] crystal direction of the single-crystalline silicon wafer. (*ii*) The KOH concentration is 29% (H_2O:KOH = 1.3:0.5 weight ratio) with a total solution of 9.6l, and the etching temperature is 80°C. At this KOH concentration and temperature the etch rate of the silicon is approximately 1.3 μm/min. (*iii*) The purity of the solution is limited by the purity of the KOH pellets supplied by the manufacturer. Maximum content of, for example, iron, cupper and nickel is in their respective order: 5, 1, and 1 ppm.

Experiment I.—After oxide stripping, ten 500 μm thick single-

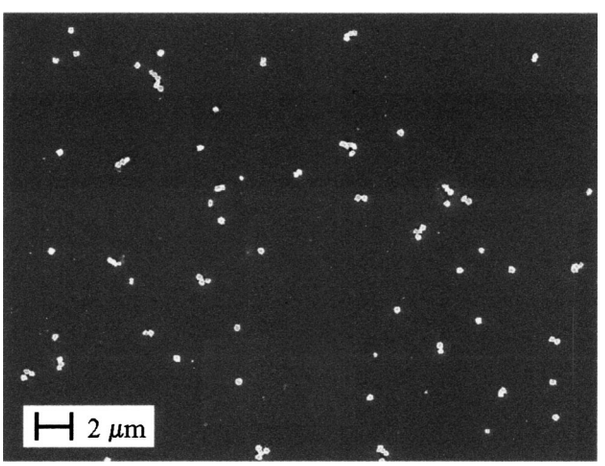

Figure 1. SEM image at 10,000 times magnification showing particles precipitated on an n-type silicon wafer.

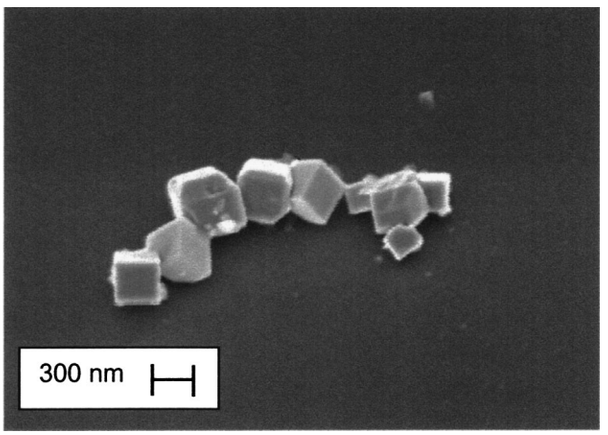

Figure 2. SEM image at a larger magnification showing particles with a cubic shape, size uniformity, and a tendency to form chains.

side polished n-type silicon (100) wafers (1-20 Ω cm) were submerged in the KOH etching solution. After 0.125, 0.25, 0.5, 1, and 2 h, respectively, two wafers were taken from the KOH solution and rinsed in deionized water for 3 min prior to a spin-drying.

Experiment II.—Four wafer types, two of each, were investigated having the following properties. Two phosphorous-doped wafers with a resistivity of 1-20 Ω cm, two antimony-doped wafers with a resistivity of less than 0.025 Ω cm, two boron-doped wafers with a resistivity of 1-20 Ω cm and two boron-doped wafers with a resistivity of less than 0.025 Ω cm. See also Table I for wafer enumeration, wafer types, and properties. After oxide stripping all wafers were etched in KOH for 30 min and subsequently rinsed as described in experiment I.

Experiment III.—As in experiment I six n-type wafers were etched for 30 min prior to rinsing and drying. After making sure that the wafers contained particles using scanning electron microscope (SEM), three of the wafers were cleaned in a 1:4 mixture of $HCl:H_2O$ solution at 24°C for 5 min, and the remaining three wafers were cleaned in a $H_2SO_4:H_2O_2$ piranha solution at 80°C for 10 min. Both batches were subsequently rinsed in deionized water with N_2 bubbling for 5 min and spin dried.

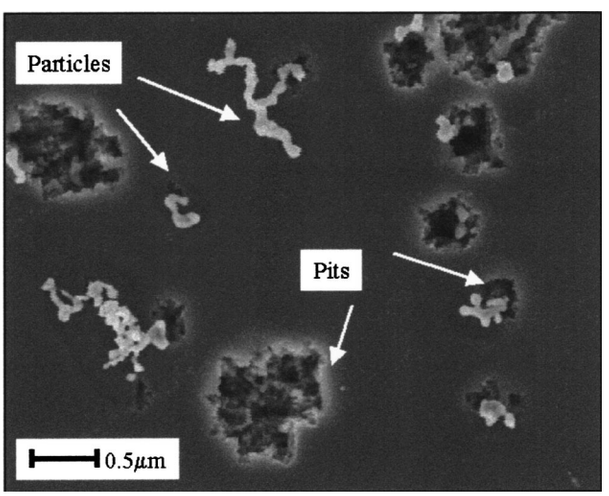

Figure 3. SEM image showing particles and etch pits in a Si membrane. The pits are caused by phosporic acid when dissolving a silicon nitride masking layer.

Table I. Wafer number and properties.

Wafer no.	Type	Dopant	Resistivity [Ω cm]	Electron/hole concentration
1-2	n	P	1-20	$\sim 4 \cdot 10^{14}$ cm^{-3}
3-4	n++	Sb	<0.025	$\sim 1 \cdot 10^{18}$ cm^{-3}
5-6	p	B	1-20	$\sim 1 \cdot 10^{15}$ cm^{-3}
7-8	p++	B	<0.025	$\sim 4 \cdot 10^{18}$ cm^{-3}

Characterization

In all the experiments the particles have been characterized in terms of morphology, quantity, and elemental composition with a LEO 1550 field emission gun SEM. In both experiment I and II the micrographs used for statistical evaluation were obtained at a magnification of 10,000 times and with a zero tilt angle of the wafers in question. The numbers presented for experiment I are a result of 19 micrographs from each sample, obtained from across the sample with a 5 mm distance between each micrograph, beginning from the flat and along an axis perpendicular to the flat as shown in Fig. 4a. In experiment II, all SEM images have been obtained at 16 predefined equidistant locations covering the whole wafer area as sketched in Fig. 4b.

Microanalysis was performed on selected particles using energy dispersive X-ray spectroscopy (EDS).

Results

Experiment I (the etching time experiment).—Figure 1 shows a typical micrograph of the precipitated particles. At larger magnifications these particular particles are recognized as cubic with a side length of approximately 330 nm as seen on Fig. 2. Typically, the particles appear in chains where the particles have the same individual size. In rare occasions the deposited particles show a hexagonal structure. In Fig. 5, one of the four particles having such a hexagonal structure is presented.

In order to perform statistical analysis on the SEM gray tone images, suitable image processing and analysis software has been used to carry out a threshold procedure that yielded binary images, *i.e.*, white particles on black wafers. The threshold images have been used to evaluate the coverage development from the bottom to the top of the wafers, to compare the coverage *vs.* etching time evolution, and to evaluate the particle size distribution on the individual wafers.

Coverage.—As stated previously image analysis has been performed on all of the obtained micrographs. Using these data, the mean value and standard deviation of the coverage for each wafer has been found for each etching time. In Fig. 6 the results from this analysis are presented. In addition, by evaluating the micrographs, two deposition modes have been recognized, in this text referred to as type I and II. Type I has a particle coverage that is lower at the

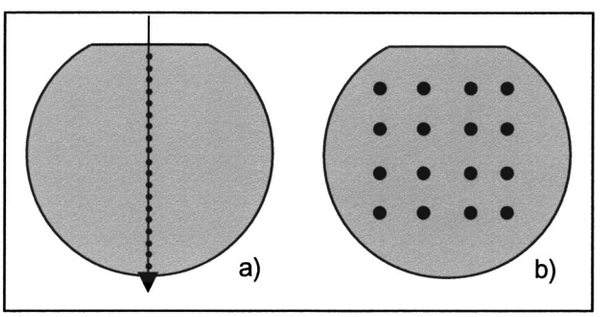

Figure 4. Schematic of the microscopy procedure. The black dots indicate where on the wafers, the SEM images were obtained.

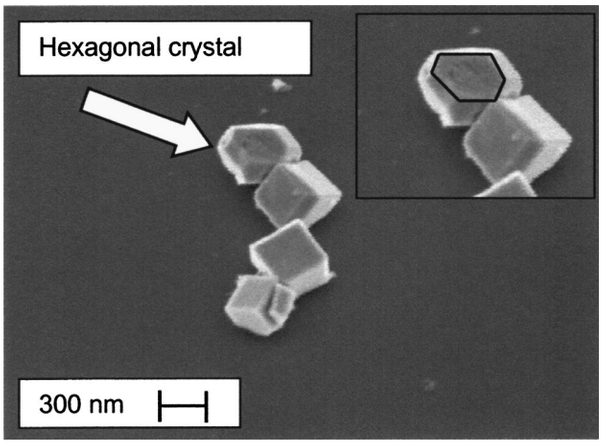

Figure 5. SEM image showing that particles in rare occasions precipitate with a hexagonal structure. The insert shows the outlined hexagonal face.

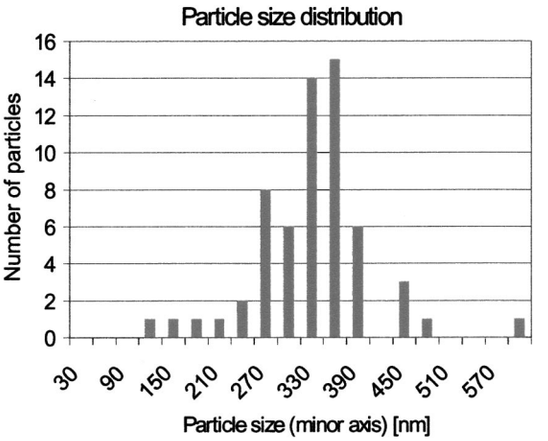

Figure 7. Histogram showing the particle size distribution as obtained from Fig. 1. The mean size of the grains is ~330 nm. The standard deviation is 75 nm, not shown in the histogram.

lower part of the wafer and higher at the upper part of the wafer. The mean coverage is low, typically 0.1%.

Type II has a coverage that is independent of the wafer coordinate and has a high overall coverage between 0.4 and 0.8%. Evaluating the mean coverage in Fig. 6 it is seen that there is no clear evolution in coverage with respect to time.

Particle size.—Size distribution analysis was performed on all micrographs obtained. The size distribution analysis corresponding to Fig. 1 is shown in Fig. 7, where it can be seen that there is a predominant particle size in the regime from 270 to 390 nm. Further, it has been found for this particular micrograph, that the mean particle size is 332 nm. Figure 7 uses the term minor axis by which is meant the thickness of the particle chain and hence a measure of the particle size. Comparing the size distribution between different etching times it was found that there was no evolution in the particle size distribution as a function of etching time.

Microanalysis was performed on a large number of particles, and it was found that they contained Fe and O. In Fig. 8 the results from a typical microanalysis are presented. At energies between 0.14 and 0.94 keV peaks corresponding to Fe and O are found. In the spectrum a peak corresponding to Si is also seen, since the analyzed particles are so small that the incoming electron beam either penetrates or is being diffracted into the Si substrate and hence yields a Si peak.

Experiment II (the wafer-type experiment).—Like experiment I, microanalysis showed that selected particles contained Fe and O. Furthermore, the n-type wafers, the p-type and the p++ type wafers showed particle coverage similar to those described in experiment I. However, highly doped n-type wafers showed an extremely different behavior. In Fig. 9 a typical SEM image from an n++ wafer is presented. Spot testing using approximately 30 particle chains from Fig. 9 yields a size distribution as shown in Fig. 10. Evaluating Fig. 10 it is seen that the chain width and thereby the particle size is quite monodispersed. Similar spot testing was performed on all wafer types. In Fig. 11 the size distribution analysis performed on the p++ type wafer is presented. Evaluating Fig. 11 it is seen that the size distribution is less narrow than in the case of the n++ type wafer. However, it can be seen that there is a strong grouping around a particle size of 220 nm. As in experiment I the coverage was found on all obtained micrographs, and the mean value and standard deviation was derived for the four different wafer types. In Fig. 12, where the resulting numbers are presented, it is seen that the n++ type wafer has a coverage which is at least 16 times higher than any other wafer type and that the other wafer types have comparable coverage, although they are different in respect to dopant type and concentration.

Experiment III.—The particle removal experiment showed that the Piranha solution dissolved most of the particles, but left what

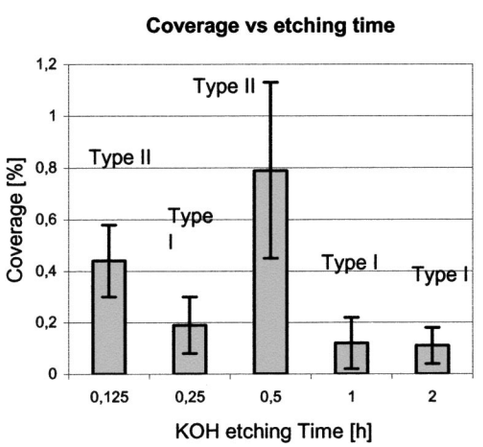

Figure 6. Histogram showing the particle coverage dependence on KOH etching time as found in experiment I.

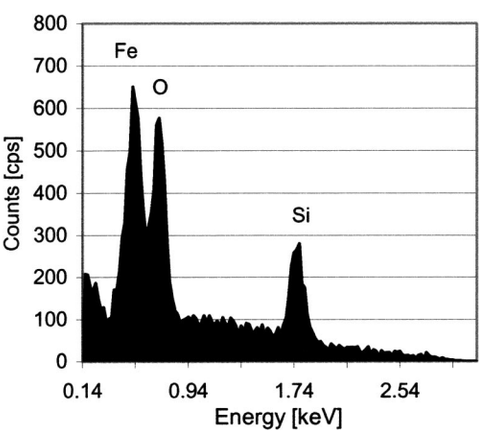

Figure 8. The results from the microanalysis of the precipitated particles. The particles are seen to contain Fe and O. The Si peak stems from the substrate.

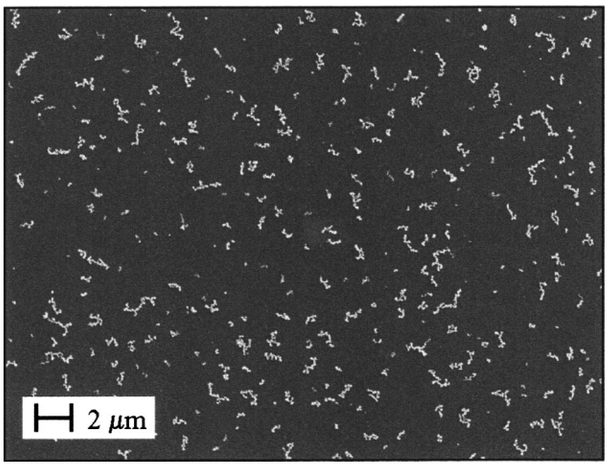

Figure 9. SEM image at 10,000 times magnification, showing particle precipitation on an n++ type silicon wafer.

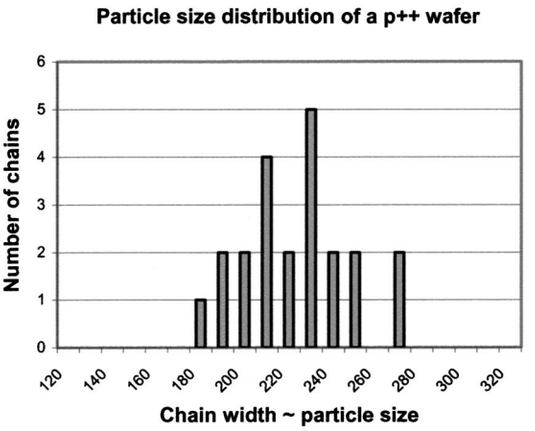

Figure 11. Histogram showing the particle size distribution as found from a spot test of the micrographs obtained from the p++ type wafers in experiment II. There is a strong grouping of particles sizes around 220 nm.

appeared to be traces of the particle chains, and that the HCl solution dissolved the particles so well it was not possible to find any using the SEM.

Discussion

Iron source.—In both experiments, EDS shows that the particles contain Fe and O. A possible iron source is the KOH pellets used for making the KOH solution. The data sheet from the KOH manufacturer states that the Fe content in the pellets is below 5 ppm. Calculations show that if the particles are for, example, hematite Fe_2O_3 then at levels of only 5 ppm in the KOH pellets, there are 1000 times more Fe ions in the solution than on the wafers.

Precipitation hypothesis.—There are several results that indicate that the precipitation phenomenon originates from an electrochemical (EC) process. This hypothesis can be elaborated in the following way. In the beginning of the etching (before 1/8 h) the Fe ions form an EC diffusion layer (DL) containing Fe complexes, in equilibrium with the solution concentration (as in Cr EC deposition[8,9] or any other case of EC deposition). However, during etching in the KOH Fe complex formation happens without particle precipitation. Then, when transferring the wafers, the EC DL sticks to the surface and from this DL, precipitation takes place either on the way to the rinsing solution or in the rising solution.

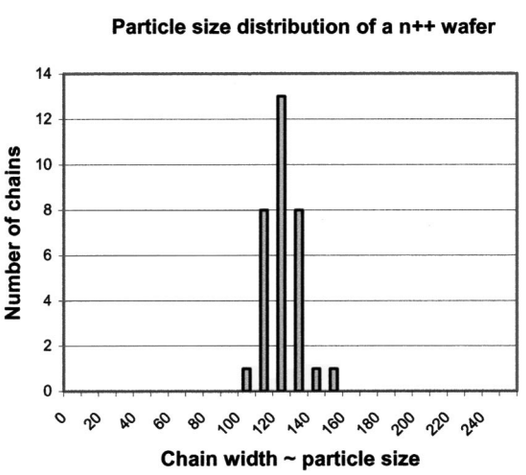

Figure 10. Histogram showing the n++ type particle size distribution as found from a spot test from Fig. 9. The mean size of the particles is ~120 nm and the standard deviation is ~10 nm.

It can be argued in the following way that the mechanism described above is in agreement with the experimental findings. First, experiment I shows that particle coverage does not increase as a function of etching time. This indicates that the precipitation stems from a finite source of Fe ions (*i.e.*, the DL) and not from an infinite Fe ion source (*i.e.*, the KOH etching solution) that otherwise would lead to an increased coverage with time. Second, experiment I also showed that there was no evolution in the particle size distribution which also suggests that there was a finite Fe source available, since the particles do not come in all sizes no matter how long time the wafers are exposed to the KOH solution, meaning that the precipitation source is the DL. Third, experiment II shows that there is a large difference in the particle size distribution between the n++ wafer (≈120 nm) and any other wafer type (≈220 nm). This suggests strongly that the particles do not come from the KOH solution as solid particles, since otherwise the particle size distribution had to be similar for all wafers. Fourth, a similar argument can be put forward regarding the differences in coverage. In experiment II, the n++ type wafer has a much higher coverage than any other wafer type. This also suggests that the particles do not come from the KOH solution as solid particles.

Precipitation, mechanism on the silicon.—According to Mori *et al.*[10] and Beverskog *et al.*[11] both the solid complex $Fe(OH)_3$ and Fe_2O_3 are theoretically stable at pH 14 and pH 12, respectively. It could therefore be argued that one or more solid phases could precipitate and subsequently adhere to the wafers during the KOH etch-

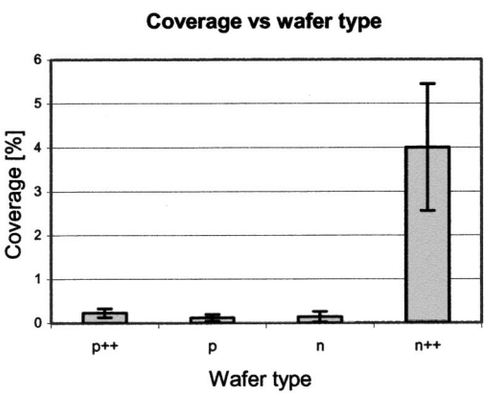

Figure 12. Histogram showing the coverage dependence on wafer types in experiment II. The n++ type wafer has a coverage that is 16 times higher than any other wafer type.

ing. In fact nanoparticles can be made intentionally using forced hydrolysis of partially neutralized $FeCl_3$ solutions with tetramethylammonium (TMAH) at pH 11.[12] However, our findings suggest that the wafer contamination source is not solid particles coming from the KOH solution.

Instead it is more likely that $Fe(OH)_3$ (aq) and $Fe(OH)_4^-$ are present in the DL. Mori *et al.*[10] have done calculations that show that at pH 14, the higher the Fe concentration the higher the $Fe(OH)^4_-$ and the $Fe(OH)_3$(aq) concentration. At this pH Mori *et al.* shows that these two hydroxide complexes are the only ones that exist. After the KOH etching the pH value and temperature drops to pH 7 and room temperature, respectively, and using these parameters the different possible species can be found in the Pourbaix diagram.[11] At $T = 25°C$ and at a pH value of 7, Fe_2O_3 (hematite) is thermodynamically stable, and therefore can be precipitated from the DL. Most of the particles found on the wafers are cubic and rarely hexagonal as should be expected since hematite has a hexagonal crystal structure. However, it has been reported before that hematite can precipitate as a pseudo-cubic crystal with (110) faces.[13-15] Therefore it cannot be ruled out that hematite is found on the wafers.

Precipitation mechanism on the silicon oxide.—The adsorbability of Fe, Ni, and Zn on silicon in a SC-1 cleaning solution (29% NH_4OH:31% H_2O_2:H_2O = 1:1:5 volume ratio) has been the subject of investigation by Mori *et al.*[10] This cleaning solution removes organic residues while oxidizing the silicon surface. In this work it has been found both experimentally using total reflection X-ray fluorescence (TRFX) spectrometry and theoretically using free energy change of adsorption calculations, that Fe will adsorb as a $Fe(OH)_3$(aq) film-type layer, instead of being adsorbed as particle-like residues on the oxidized silicon surface. These results were found for pH 11 and at a temperature of 80°C. Mori *et al.*[10] have also performed calculations that compare the free energy change of adsorption for $Fe(OH)_x$ (x = 0 to 4) as a function of pH (0-14). Mori *et al.* find that $Fe(OH)_3$(aq) yields the least calculated free energy change of adsorption, hence substantiating that, in the case of KOH etching, iron adsorbs the silicon oxide surface in the form of $Fe(OH)_3$(aq). In this work Mori *et al.* also established an adsorbed Fe surface concentration saturation point. Our findings regarding the lack of precipitation on the silicon oxide mask are in agreement with these findings of the Fe surface concentration. Mori *et al.* have experimentally shown using TRXF, that the surface metal concentration depends linearly on the Fe molar concentration in a log-log plot between 10^{-9} and 10^{-7} mol L^{-1}. Above 10^{-7} mol L^{-1} the surface metal concentration does not go much above $2 \cdot 10^{13}$ atom cm^{-2}. In our experiment, with an assumed contamination level of 5 ppm of Fe in the KOH, the concentration of Fe ions in the solution is $\sim 4 \cdot 10^{-5}$ mol L^{-1} This means that the Fe molar concentration is so high that the saturation point, found by Mori *et al.*[10] has been reached. In the case of the n++ type wafers, the coverage contamination is, in the worst case, 4%. Assuming that all the particles are cubic, with a side length of 120 nm, it is found that the surface metal concentration before precipitation would be $3.2 \cdot 10^{-8}$ mol cm^{-2} or $2 \cdot 10^{16}$ atom cm^{-2}. This is 1000 times more than the saturation point found by Mori *et al.*[10] This fact indicates that, if there is a saturation point in the case of etching of Si in KOH, it is at least 1000 times higher than in the case of SC-1. The low contamination level of the silicon oxide due to saturation makes it difficult to characterize the contamination using SEM. Additionally it should be pointed out that a surface metal concentration of $2 \cdot 10^{16}$ atom cm^{-2} corresponds to 200 atom nm^{-2} which is not possible in one atomic surface layer and therefore it must be assumed that the Fe must be contained in the EC DL in whatever complex the iron has formed.

In earlier papers it has been shown using electron reflection diffractometry[16,17] and photometry[7] that a layer of metallic iron can adsorb on silicon after KOH etching, with a thickness up to 50 Å. This high level of contamination corresponds well to our findings in case of the n++ type wafers.

The difference in coverage between n++ type wafers and any other wafer types was found to be significant. The reason for this phenomenon is still unclear. Clearly it has to do with the dopant type and dopant level, because it is the wafer with the highest electron concentration that yields the highest coverage. As shown in Table I, the n-type wafer has an electron concentration of $4 \cdot 10^{14}$ cm^{-3} and the n++ type wafer has an electron concentration of 10^{18} cm^{-3}. Future work on this phenomenon should investigate coverage as a function of electron concentration in the electron density regime between $4 \cdot 10^{14}$ and 10^{18} cm^{-3} and at higher concentrations.

Conclusions

The precipitation of Fe_xO_y particles on Si wafers in connection with KOH etching has been investigated, and it has been shown that there is no significant change in the amount of particle coverage of the silicon wafers with respect to etching time. The amount of deposited material is wafer-type dependent, *i.e.*, n++ wafers show a coverage that is at least 16 times higher than on any other wafer type investigated. Furthermore, it has been found for all wafer types that the precipitated particles have a size distribution with a predominant size regime and that this size regime is different for different wafer types. The experimental findings suggest that the precipitation is taking place after the KOH etching, but that the source of the precipitation is the electrochemical double layer formed during the KOH etching procedure. The particles that causes etch pits on the Si surface when exposed to a phosphoric acid solution can successfully be removed in a dilute HCl solution.

Acknowledgments

This work was made possible within the SUM project for development of microsystem products in the industrial collaboration between DELTA Dansk Elektronik, Lys & Akustik, Danfoss A/S, Grundfos A/S, Sonion MEMS A/S (former Microtronic A/S), Capres A/S, and Mikroelektronik Centret. The project is supported by the Danish Agency for Trade and Industry and the Danish Research Agency.

The Technical University of Denmark assisted in meeting the publication costs of this article.

References

1. R. de Reus, C. Christensen, S. Weichel, S. Bouwstra, J. Janting, G. F. Eriksen, K. Dyrbye, T. R. Brown, J. P. Krog, O. S. Jensen, and P. Gravesen, *Microelectron. Reliab.*, **38**, 1251 (1998).
2. A. A. Istratov, H. Hieslmair, and E. R. Weber, *Appl. Phys. A: Solids Surf.*, **70**, 489 (2000).
3. H. Tanaka, Y. Abe, T. Yoneyama, J. Ishikawa, O. Takenaka, and K. Inoue, *Sens. Actuators B*, **82**, 270 (2000).
4. A. Hein, Q. Dorsch, and E. Obermeier, in *Proceedings of International Solid State Sensors and Actuators Conference (Transducers '97)* **1**, 687 (1997).
5. S. A. Campbell, K. Cooper, L. Dixon, R. Earwaker, S. N. Port, and D. J. Schiffrin, *J. Micromech. Microeng.*, **5**, 209 (1995).
6. Y. Hirata, M. Tsugai, K. Tanimoto, T. Usami, Y. Yamaguchi, H. Otani, and K. Nakamura, *Proc. SPIE*, **3874**, 276 (1999); *SPIE the International Society for Optical Engineering*.
7. M. Neubert and B. Nippe, *Cryst. Res. Technol.*, **26**, K203 (1991).
8. P. Leisner, Ph.D. Thesis, The Technical University of Denmark, Lyngby, Denmark (1992).
9. C. B. Nielsen, P. Leisner, and A. Horsewell, *J. Appl. Electrochem.*, **28**, 141 (1998).
10. Y. Mori, K. Uemura, and K. Shimanoe, *J. Electrochem. Soc.*, **142**, 3104 (1995).
11. B. Beverskog and I. Puigdomenech, *Corros. Sci.*, **38**, 2121 (1996).
12. S. Musić, I. Czakó-Nagy, I. Salaj-Obelić, and N. Ljubešić, *Mater. Lett.*, **32**, 301 (1997).
13. A. H. Morrish, *Canted Antiferromagnetism: Hematite*, p. 7, World Scientific, Singapore (1994).
14. S. Sato, Y. Harada, Y. Waseda, and T. Sugimoto, *Rev. Laser Eng.*, **24**, 1193 (1996).
15. S. Manjun, *Acta Metall. Sin.*, **36**, 230 (2000).
16. P. J. Holmes and R. C. Newman, in *Proceedings of the Institute of Electrical Engineers. B*, 106, Suppl. 15, p. 287 (1956).
17. P. J. Holmes and R. C. Newman, Paper 2998 E, in *Proceedings of the Institute of Electrical Engieners*. p. 287 (1960).